# Electronic Supplementary Information

## Heterogeneous Catalase-like Activity of Gold(I)-Cobalt(III) Metallosupramolecular Ionic Crystals

**M. Yamada,[a] N. Yoshinari,[a] N. Kuwamura,[a] T. Saito,[b] S. Okada,[c] S. P. Maddala,[c] K. Harano,[c] E. Nakamura,[c] K. Yamagami,[d] K. Yamanaka,[e] A. Sekiyama,[d] T. Suenobu,[f] Y. Yamada,[g] and T. Konno*[a]**

[a]Department of Chemistry, Graduate School of Science, Osaka University, Toyonaka, Osaka 560-0043 (Japan)
Fax: (+81) 6-6850-5765
E-mail: konno@chem.sci.osaka-u.ac.jp

[b]Department of Biomedical Information Science, Graduate School of Information Science, Hiroshima City University, Asa-Minami-ku, Hiroshima 731-3194 (Japan)

[c]Department of Chemistry, Graduate School of Science, The University of Tokyo, Bunkyo-ku, Tokyo, 113-0033 (Japan)

[d]Division of Materials Physics, Graduate School of Engineering Science, Osaka University, Toyonaka, Osaka 560-8531 (Japan)

[e]Synchrotron Radiation Center, Ritsumeikan University, Kusatsu, Shiga 525-8577 (Japan)

[f]Department of Material and Life Science, Graduate School of Engineering, Osaka University, ALCA and SENTAN, Japan Science and Technology (JST), Suita, Osaka 565-0871 (Japan)

[g]Department of Applied Chemistry & Bioengineering, Graduate School of Engineering, Osaka City University, 3-3-138 Sugimoto, Sumiyoshi-ku, Osaka 558-8585 (Japan)

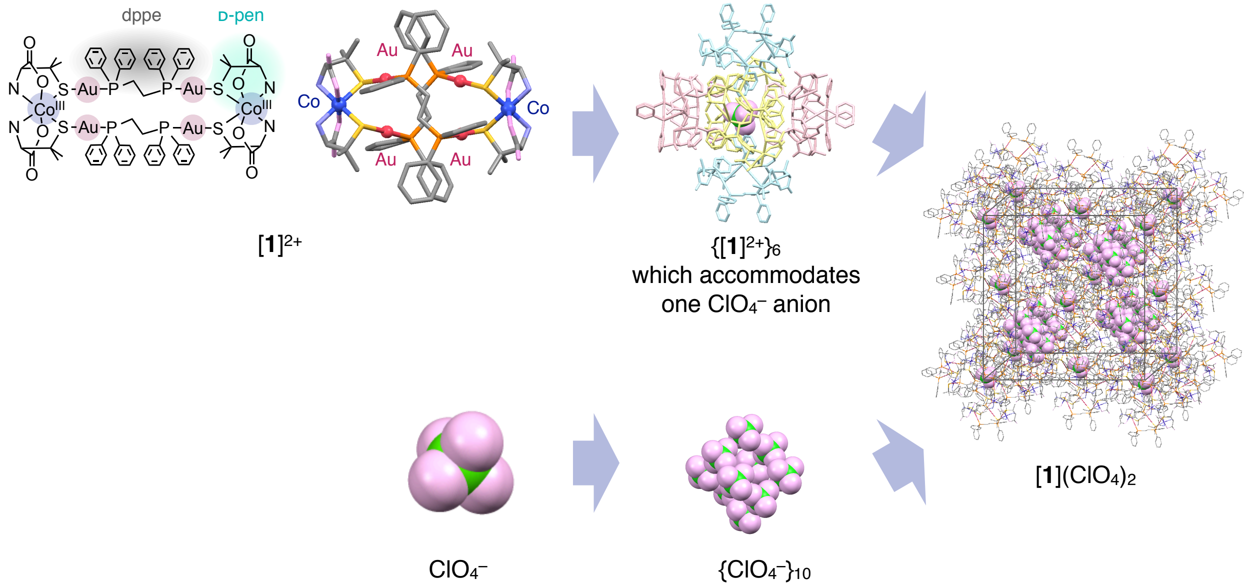

**Fig. S1** Schematic figure of the formation of $[\mathbf{1}](ClO_4)_2$. $H_2O$ molecules are omitted for clarity.

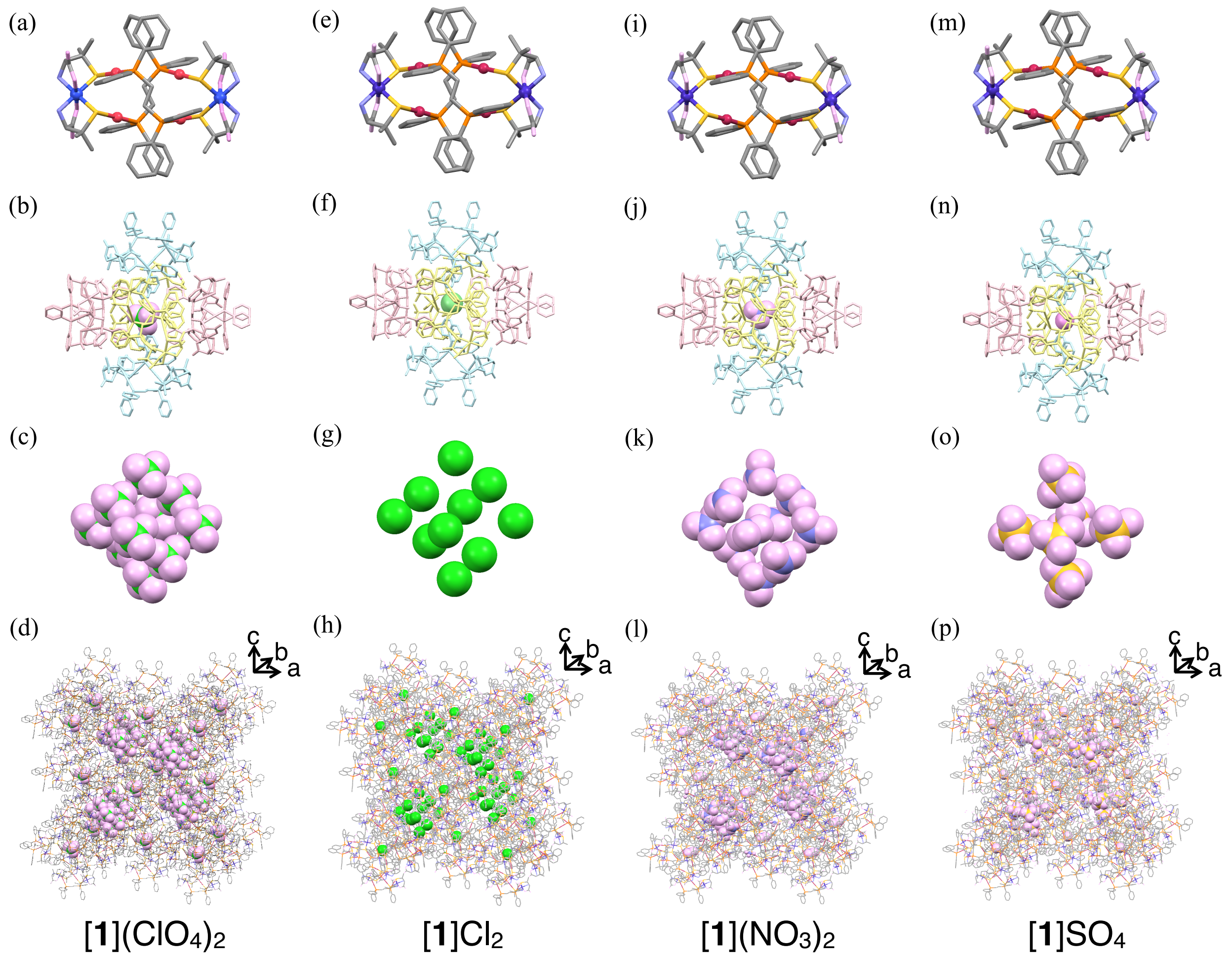

**Fig. S2** Structures of (a, e, i, m) complex cations, (b, f, j, n) octahedron-shaped cationic supramolecules $\{[\mathbf{1}]^{2+}\}_6$ accommodating an anion, (c, g, k) adamantane-shaped anionic clusters $\{X^-\}_{10}$ and (o) octahedron-shaped anionic clusters $\{X^{2-}\}_6$ and (d, h, l, p) the packing structure of $[\mathbf{1}](ClO_4)_2$, $[\mathbf{1}]Cl_2$, $[\mathbf{1}](NO_3)_2$, and $[\mathbf{1}]SO_4$, respectively.

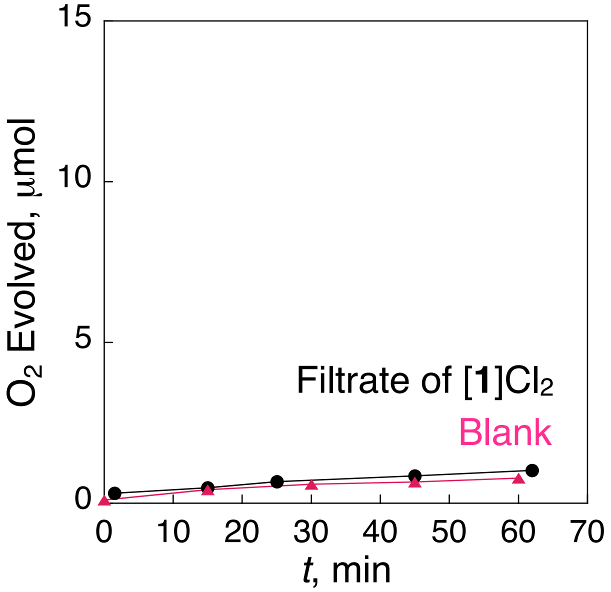

**Fig. S3** Time profiles of the evolution of $O_2$ from the filtrate of [**1**]$Cl_2$ (1 mL) (black circles) and 5 wt% aqueous $H_2O_2$ (1 mL) (pink triangles) at 298 K. The filtrate of [**1**]$Cl_2$ was prepared by the following procedure; the catalytic amount of crystals of [**1**]$Cl_2$ (4.7 mg, approximately 1.0 × 1.0 × 1.0 mm) was soaked in a 5 wt% aqueous $H_2O_2$ (1 mL) and filtered after 20 min.

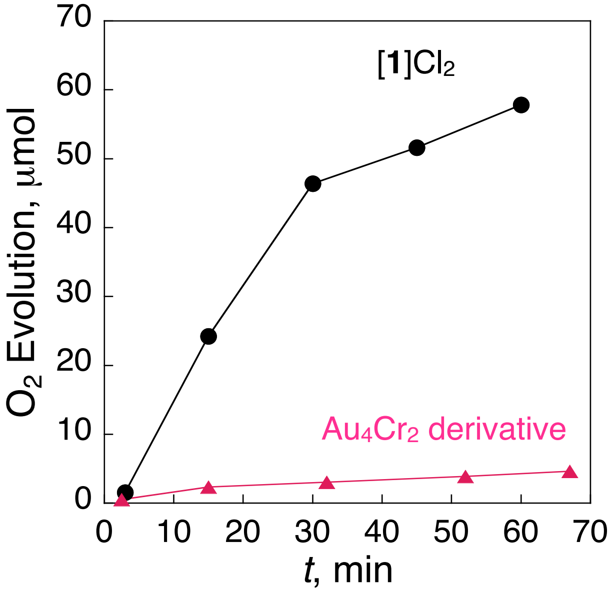

**Fig. S4** Time profiles of the evolution of $O_2$ during treatment with a catalytic amount of [**1**]$Cl_2$ (5.0 mg, approximately 0.5 × 0.5 × 0.5 mm) and the $Au_4Cr_2$ derivative [$Au_4Cr_2$(dppe)$_2$(D-pen)$_4$]$Cl_2$ (5.2 mg, approximately 0.05 × 0.05 × 0.05 mm) with 5 wt% aqueous $H_2O_2$ (1.00 mL) at 298 K.

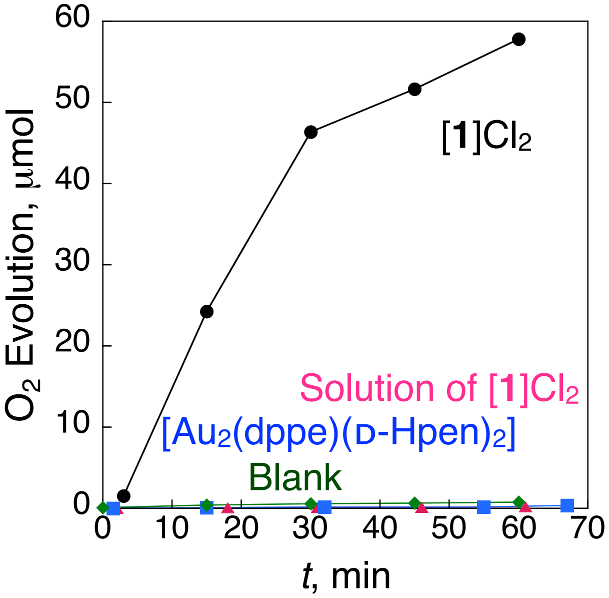

**Fig. S5** Time profiles of the evolution of $O_2$ in the disproportionation of 5 wt% aqueous $H_2O_2$ with a catalytic amount of crystals of [**1**]$Cl_2$ (5.0 mg, approximately 0.5 × 0.5 × 0.5 mm), a saturated homogeneous solution of [**1**]$Cl_2$ and a metalloligand [$Au_2$(dppe)(D-Hpen)$_2$] (5.2 mg) and without the addition of any metal complex in $H_2O$ (1.00 mL) at 298 K.

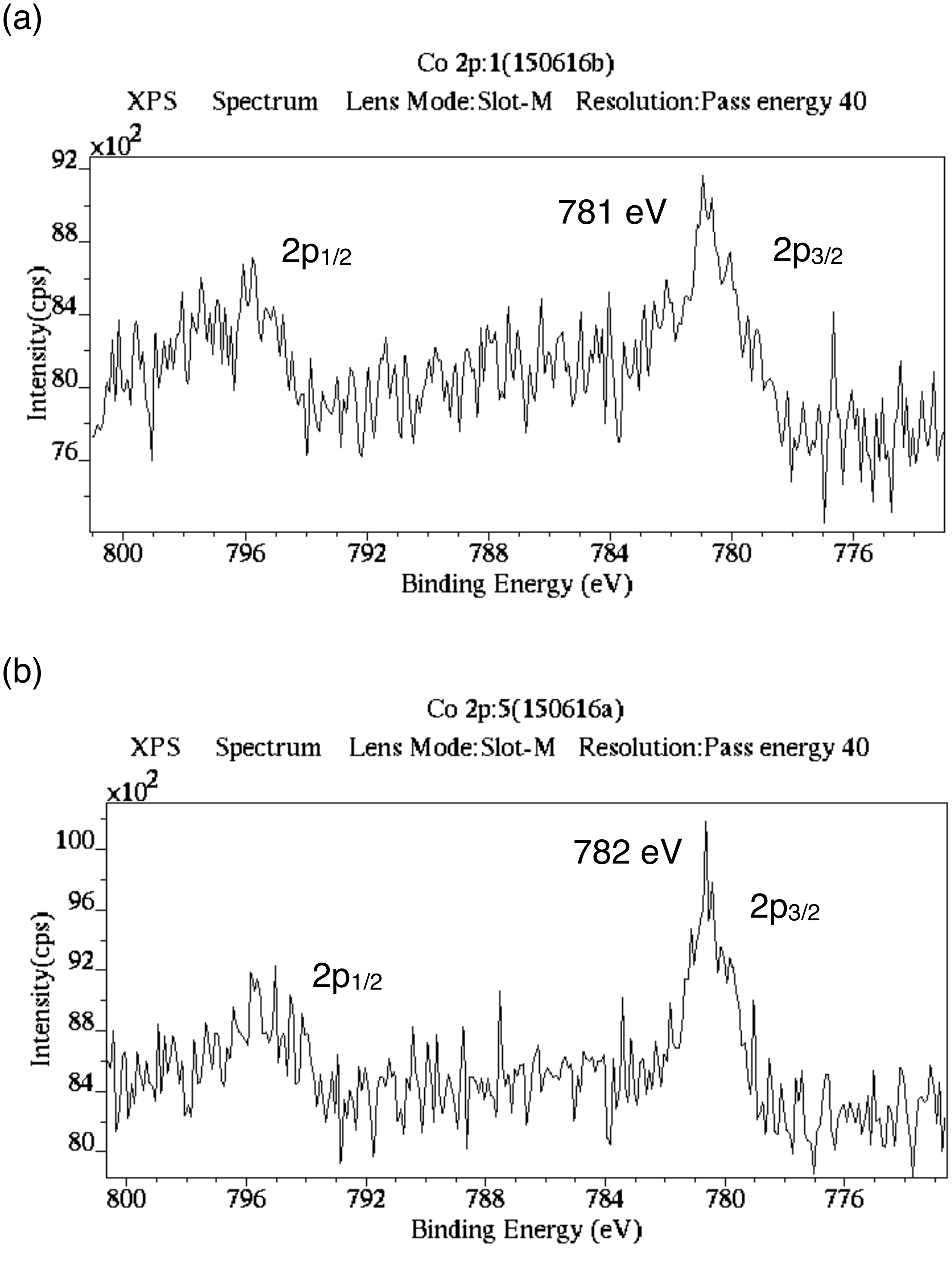

**Fig. S6** XPS of [**1**]Cl$_2$ (a) before and (b) after reaction with H$_2$O$_2$ for 15 min.

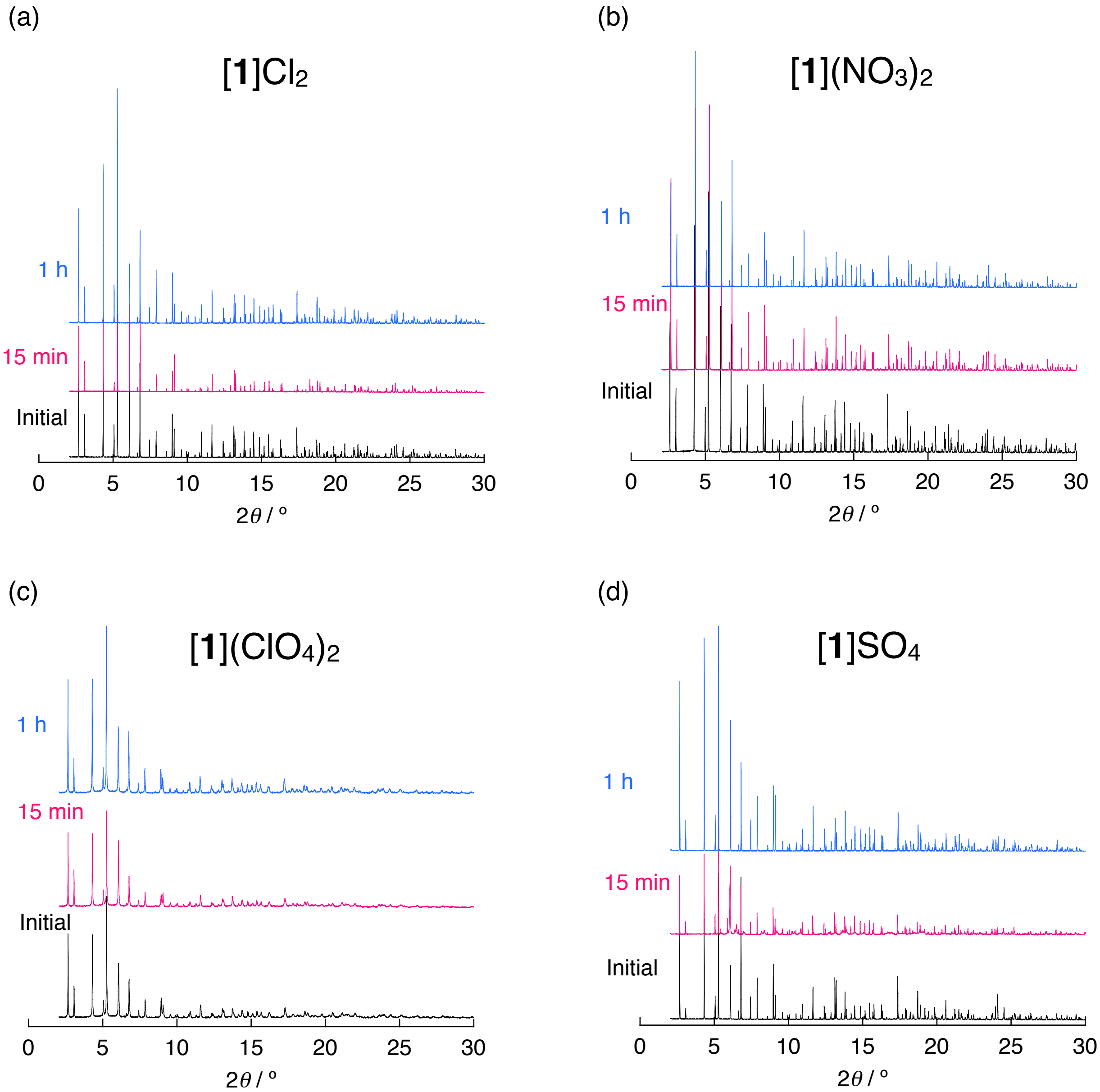

**Fig. S7** Powder XRD patterns of the initial samples and samples reacted with $H_2O_2$ for 15 min or 1 h for (a) [**1**]$Cl_2$, (b) [**1**]$(NO_3)_2$, (c) [**1**]$(ClO_4)_2$ and (d) [**1**]$SO_4$.

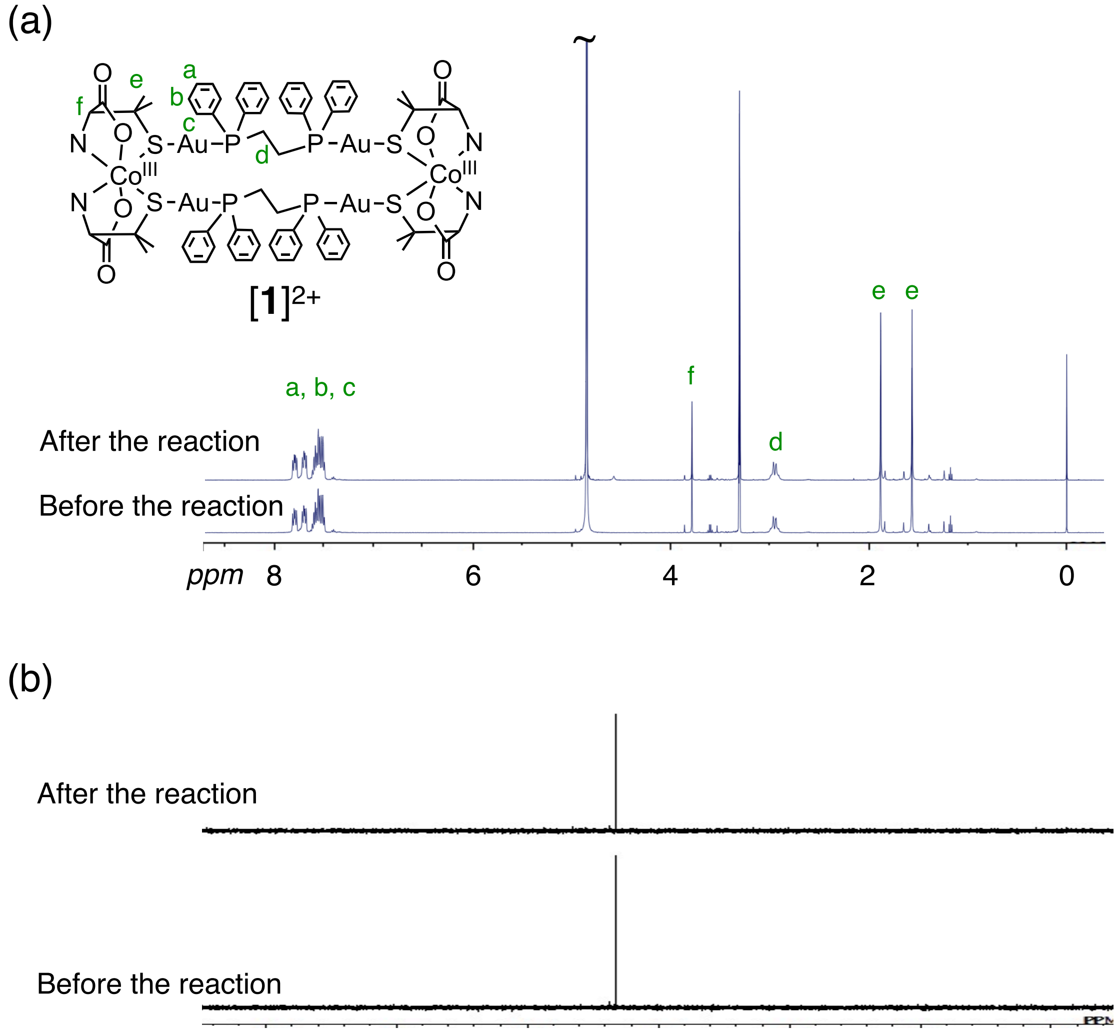

**Fig. S8** (a) $^1$H and (b) $^{31}$P NMR spectra (500 MHz for $^1$H and 202 MHz for $^{31}$P, methanol-*d*$_4$, 298 K) of [**1**]Cl$_2$ before and after reaction with $H_2O_2$ for 15 min.

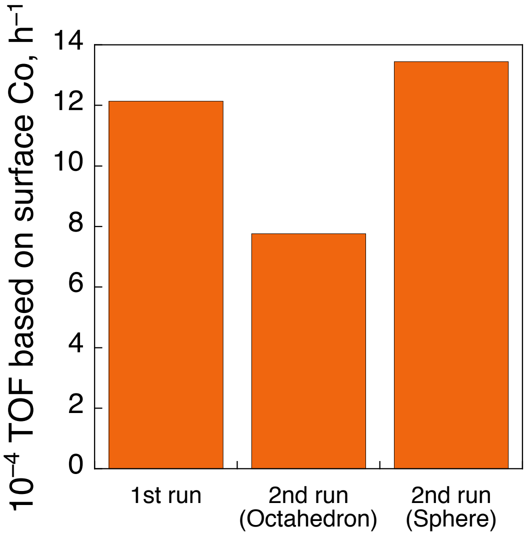

**Fig. S9** TOF ($h^{-1}$) calculated based on the surface Co atoms at 15 min in the disproportionation of 5 wt% aqueous $H_2O_2$ with [**1**]$Cl_2$ (1st: 5.2 mg, 1.0 × 1.0 × 1.0 mm; 2nd: 4.6 mg, 0.3 × 0.3 × 0.3 mm) in $H_2O$ (1.00 mL) at 298 K in the first run and second run. In the second run, the calculation was carried out with an approximation of the complete octahedral crystal in the initial state and the complete spherical crystal with the lowest specific surface area to show a possible range because the crystals obtained after the first run were not complete octahedrons due to partial cracking.

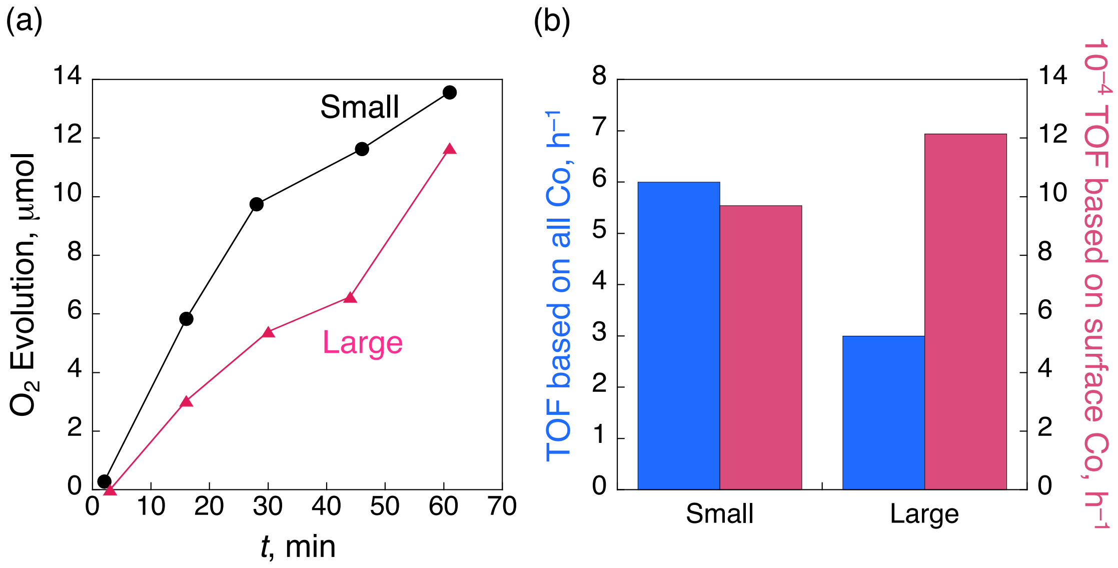

**Fig. S10** (a) Time profiles of the evolution of $O_2$ in the disproportionation of 5 wt% aqueous $H_2O_2$ with a catalytic amount of small crystals (5.2 mg, 0.4 × 0.4 × 0.4 mm) and large crystals (5.2 mg, 1.0 × 1.0 × 1.0 mm) of [**1**]$Cl_2$ in $H_2O$ (1.00 mL) at 298 K and (b) the TOF calculated based on all the Co atoms or the surface Co atoms at 15 min.

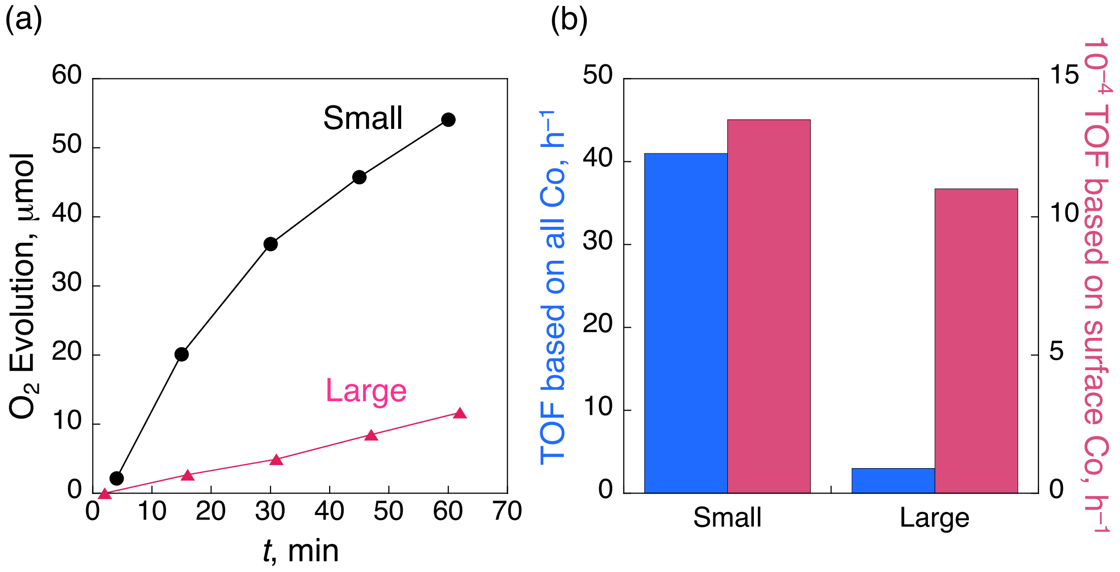

**Fig. S11** (a) Time profiles of the evolution of $O_2$ in the disproportionation of 5 wt% aqueous $H_2O_2$ with a catalytic amount of small crystals (4.9 mg, 0.05 × 0.05 × 0.05 mm) and large crystals (5.1 mg, 1.0 × 1.0 × 1.0 mm) of [**1**]$(NO_3)_2$ in $H_2O$ (1.00 mL) at 298 K and (b) the TOF calculated based on all the Co atoms or the surface Co atoms at 15 min.

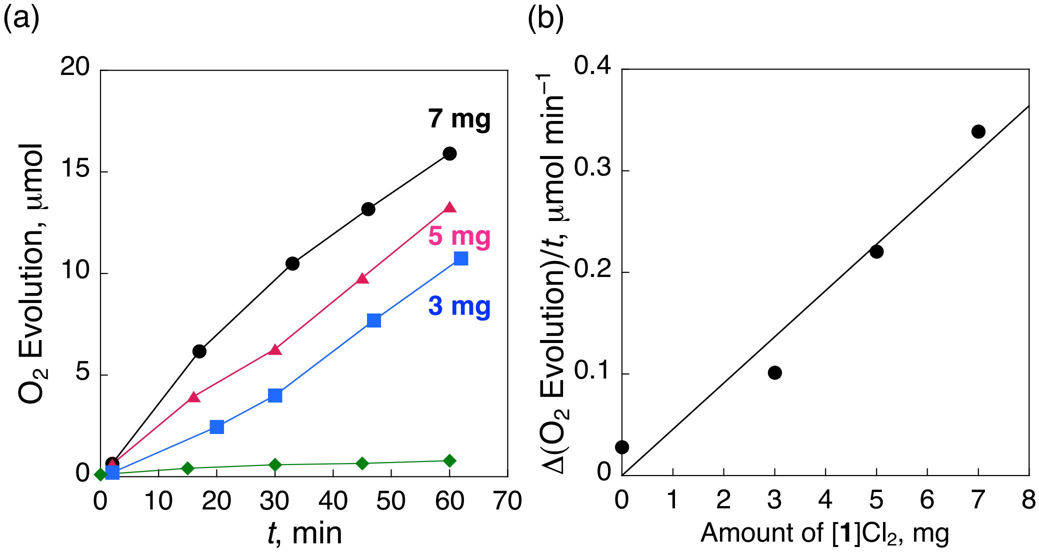

**Fig. S12** (a) Time profiles of the evolution of $O_2$ in the disproportionation of 5 wt% aqueous $H_2O_2$ with various amounts of 1.0 × 1.0 × 1.0 mm-sized crystals of [**1**]$Cl_2$ (3.0, 4.8, 7.6 and 0 mg) in $H_2O$ (1.00 mL) at 298 K and (b) the dependence on the amount of [**1**]$Cl_2$ of the initial rate of evolution of $O_2$, Δ($O_2$ evolution)/*t*, calculated at 15 min .

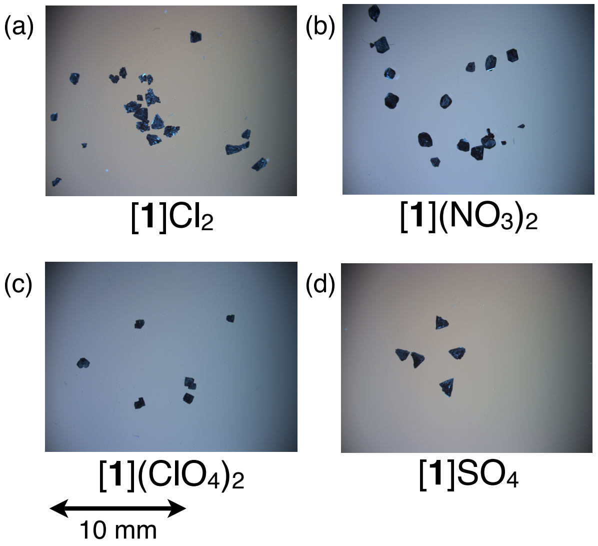

**Fig. S13** Microscopic photos of crystals of (a) [**1**]$Cl_2$, (b) [**1**]$(NO_3)_2$, (c) [**1**]$(ClO_4)_2$ and (d) [**1**]$SO_4$ used for the reaction.

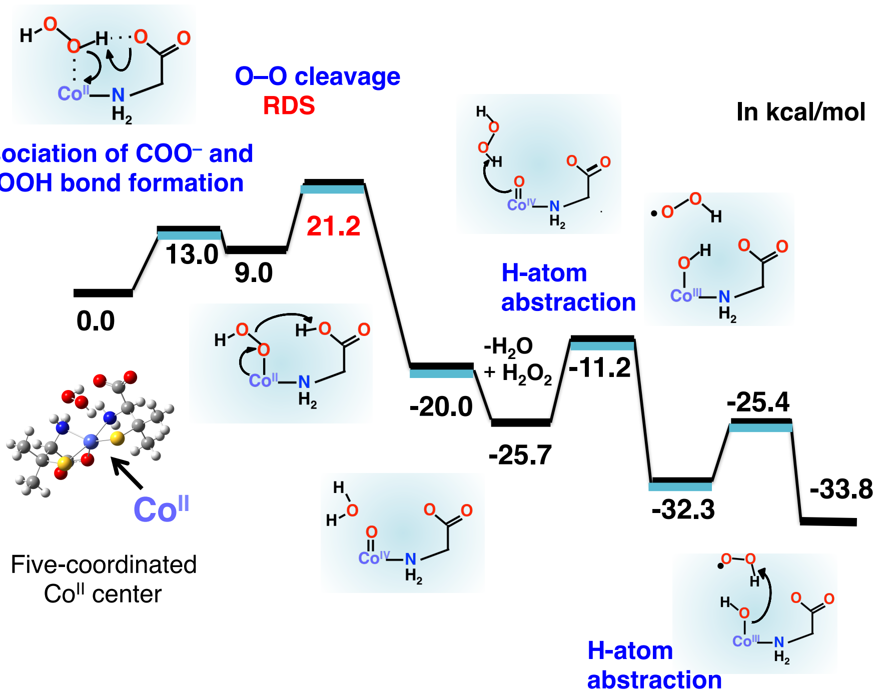

**Fig. S14** Energy profile of the proposed mechanism from a five-coordinated $Co^{II}$ center. Optimization of the models and calculation of the relative energies (in kcal/mol) were performed at the UB3LYP-D/6-31G$^*$ level.

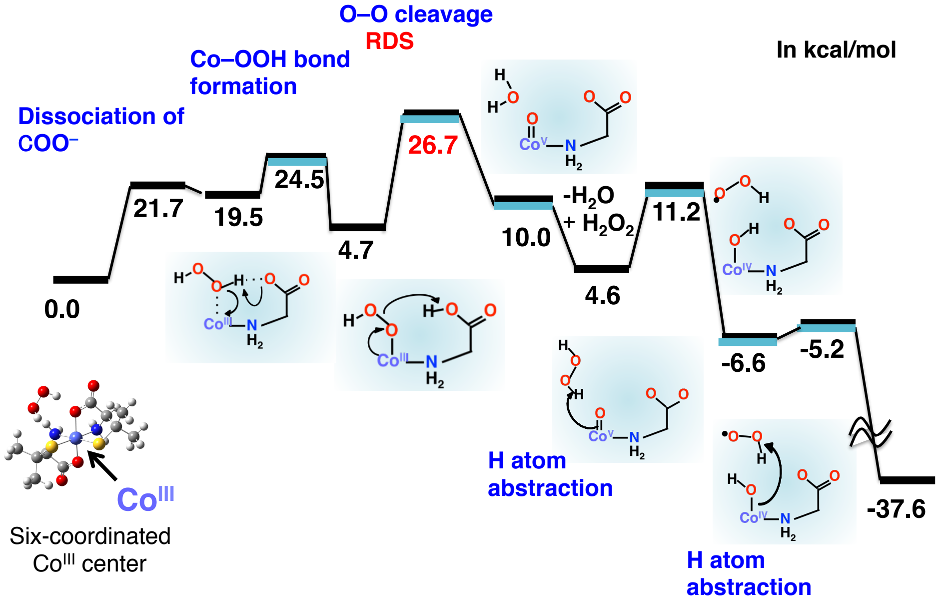

**Fig. S15** Energy profile of the proposed mechanism starting from a six-coordinated $Co^{III}$ center. Optimization of the models and calculation of the relative energies (in kcal/mol) were performed at the UB3LYP-D/6-31G$^*$ level.

**Table S1** Concentrations of saturated aqueous solutions of [**1**]$X_n$ estimated from UV-vis spectra based on the molar absorption coefficient of [**1**]$Cl_2$ in a methanol solution.

| Compound | Solubility |
|---|---|
| $[Au^I_4Co^{III}_2(dppe)_2(\text{D-pen})_4]Cl_2$ | 0.18 mM |
| $[Au^I_4Co^{III}_2(dppe)_2(\text{D-pen})_4](NO_3)_2$ | < 0.01 mM |
| $[Au^I_4Co^{III}_2(dppe)_2(\text{D-pen})_4](ClO_4)_2$ | 0.11 mM |
| $[Au^I_4Co^{III}_2(dppe)_2(\text{D-pen})_4]SO_4$ | 1.4 mM |

**Table S2** Concentrations of leached Co and Au in the reaction mixture at 20-30 min detected by ICP-AES after filtration of the crystals [1]$X_n$. The reaction conditions are similar to the reactions for GC measurements: 5 wt% aqueous $H_2O_2$ with a catalytic amount of crystals of [**1**]$Cl_2$ (75.0 mg, approximately 1.0 × 1.0 × 1.0 mm) or [**1**]$(NO_3)_2$ (74.9 mg, approximately 1.0 × 1.0 × 1.0 mm) in $H_2O$ (15.0 mL) at 298 K.

| Compound | Concentration of Co (Leached crystal ratio) | Concentration of Au (Leached crystal ratio) |
|---|---|---|
| $[Au^I_4Co^{III}_2(dppe)_2(\text{D-pen})_4]Cl_2$ | 0.435 ppm<br>(0.188%) | 1.99 ppm<br>(0.128%) |
| $[Au^I_4Co^{III}_2(dppe)_2(\text{D-pen})_4](NO_3)_2$ | 0.052 ppm<br>(0.023%) | 0.25 ppm<br>(0.016%) |

**Table S3** Representatives of the reported catalase-like activities.

| Catalyst | Catalytic activity[d] | Conditions |
|---|---|---|
| Typical heme catalases[a] | TOF =<br>$5.4 \times 10^4 \sim 83.3 \times 10^4\ s^{-1}$ | various |
| $MnO_2$[b] | $k = 2.3 \times 10^4\ s^{-1}$ | rt, $[H_2O_2] = 0.50$ M,<br>$MnO_2$ (50 mg) in 250 mL reactor,<br>at 0-100 min |
| $K_2Cr_2O_7$[b] | $k = 1.2 \times 10^4\ s^{-1}$ | rt, $[H_2O_2] = 0.50$ M,<br>$K_2Cr_2O_7$ (50 mg) in 250 mL reactor,<br>at 0-100 min |
| $Co(HPHOPD)_2$[c] | TOF = $5.5 \times 10^3\ h^{-1}$ | 308 K, $[H_2O_2] = 5$ vol,<br>$Co(HPHOPD)_2$ (40 mg) in 10 mL,<br>at 10 min |
| [**1**]$Cl_2$ | TOF = $1.2 \times 10^5\ h^{-1}$<br>(= ~$3.3 \times 10\ s^{-1}$)<br>$k = 8.0\ s^{-1}$ | rt, $[H_2O_2] = 5\%$,<br>[**1**]$Cl_2$ (5 mg) in 1 mL,<br>at 15 min |
| [**1**]$(NO_3)_2$ | TOF = $1.4 \times 10^5\ h^{-1}$<br>(= ~$3.9 \times 10\ s^{-1}$)<br>$k = 8.2\ s^{-1}$ | rt, $[H_2O_2] = 5\%$,<br>[**1**]$(NO_3)_2$ (5 mg) in 1 mL,<br>at 15 min |

[a] J. Switala and P. C. Loewen, *Arch. Biochem. Biophys.*, 2002, **401**, 145–154; J. Vlasits, C. Jakopitsch, M. Bernroitner, M. Zamocky, P. G. Furtmüller and C. Obinger, *Arch. Biochem. Biophys.*, 2010, **500**, 74–81. [b] M.A. Hasnat, M. M. Rahman, S.M. Borhanuddin, A. Siddiqua, N.M. Bahadur and M.R. Karim, *Catal. Comm.*, 2010, **12**, 286–291. [c] HOHOPD = 2-oximinopropanedione, R. V. Prasad and N. V. Thakkar, *J. Mol. Catal.*, 1994, **92**, 9–20. [d] The values of TOF and $k$ were calculated as $V/[\text{catalyst}]$ and $2V/[H_2O_2]$, where $V = O_2$ evolution rate.